

X-exoplanets: an X-ray and EUV database for exoplanets

J. Sanz-Forcada¹, D. García-Álvarez^{2,3}, A. Velasco^{1,4}, E. Solano^{1,4},
I. Ribas⁵, G. Micela⁶ and A. Pollock⁷

¹Centro de Astrobiología, CSIC-INTA, European Space Astronomy Center
Apartado 78, E-28691 Villanueva de la Canada (Madrid), Spain
email: jsanz@cab.inta-csic.es

²Instituto de Astrofísica de Canarias, Spain

³Grantecan CALP, Spain

⁴Spanish Virtual Observatory, Spain

⁵Institut de Ciències de l'Espai (CSIC-IEEC), Spain

⁶INAF- Osservatorio Astronomico di Palermo, Italy

⁷XMM-Newton SOC, European Space Agency, ESAC, Spain

Abstract. Extreme Ultraviolet (EUV) and X-ray emission is of great importance in several phenomena related to the formation of planetary systems and the atmospheres of planets. The atmospheric composition, and the mass of an exoplanet, are partly dependent on the X-ray and EUV radiation received during the first stages of formation and even during main sequence of the star. Biological life developing on exoplanets would depend severely on the high energy radiation arriving from its parent star.

Here we present a database of the X-ray and EUV emission of all the stars currently known to host exoplanets. The archive is public and accessible through the Spanish Virtual Observatory (SVO). The database gives the user the option to download observed X-rays and EUV spectra. Synthetic spectra covering the spectral range 1–912 Å are also available (present day telescopes do not give access to the EUV range at $\lambda > 180$ Å). These spectra are created using coronal models after fitting observed spectra.

Keywords. astrobiology, (stars:) planetary systems, stars: coronae, stars: abundances, X-rays: stars, atomic data

1. Introduction

Since the discovery of the first transiting exoplanet, it has been proposed that high energy stellar radiation should have some influence on the atmosphere of the planets (e.g. Seager & Sasselov 2000), in special the so called “hot Jupiters”, planets with Jupiter-like mass at a short distance of the star. The effects of the high energy radiation (UV, EUV and X-rays) are important at different stages. First, during protoplanetary disc dissipation. Later, when the stellar rotation is fast and the planet keeps most of its original atmosphere, this radiation is believed to be a strong erosive agent for the atmosphere (e.g. Lammer *et al.* 2003). Finally, the developing of biological life in a planet will partly depend on the high energy (EUV and UV in special) radiation arriving to the surface.

During the evolution of a planet we have to consider also the evolution of its parent star. Once the protostellar disc dissipates, the rotation of the star will progressively slows down. The initial strong stellar rotation produces high coronal activity, with EUV and X-rays emission from the material heated at 1–30 MK. About ~100 Myr after the stellar birth, the X-rays and EUV emission flux from the corona decreases and cools down, as

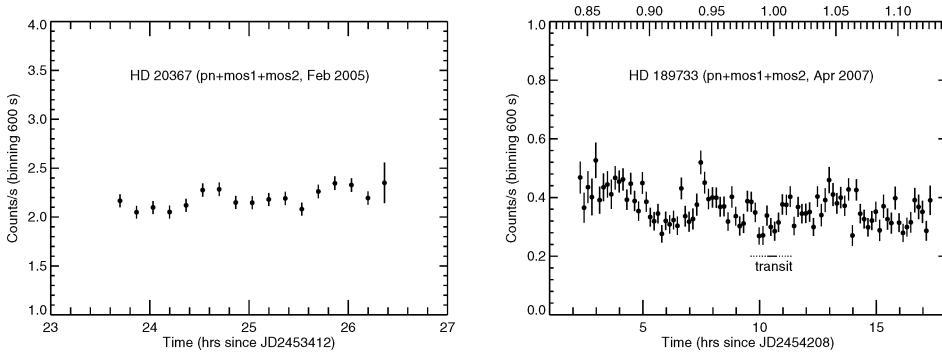


Figure 1. Two examples of X-ray light curves with some variability. *Left:* HD 20367, one of the most active stars in the sample. *Right:* HD 189733 hosts a transiting planet. The times for the total and partial (optical) transit are displayed, Upper axis show the orbital phase of the planet. Observations of evaporation signatures have been reported for this planet (Tinetti *et al.* 2007). High energy radiation is essential in this effect.

an effect of the slower rotation. The UV emission from the chromosphere and transition region follows the same pattern with age. It is possible to test the X-ray evolution with time by looking at the stellar clusters (Micela 2002). A direct application to the solar case was proposed by Ribas *et al.* (2005). A more detailed coronal model was employed by Clossen *et al.* (2007) to evaluate the spectral energy distribution of κ Cet, a proxy of the Sun at the time in which life developed on Earth.

In the last years there has been an increasing interest in the use of the high energy emission from the parent star to know the possible effects on the planet, such as vaporization or atmospheric “erosion” (Lammer *et al.* 2003; Baraffe *et al.* 2004; Erkaev *et al.* 2007; Penz & Micela 2008; Penz *et al.* 2008; Cecchi-Pestellini *et al.* 2009; Lammer *et al.* 2009, Sanz-Forcada *et al.*, submitted). These models are limited to the use of X-ray or EUV fluxes calculated in the whole band. The use of a spectral energy distribution, with the highest resolution achievable, would be preferred to know better the effects in the planet atmosphere. The access to high resolution spectra in this spectral range is, however, very limited. For X-rays there are currently two large telescopes (XMM-Newton and Chandra) providing the ranges $\sim 4 - 38 \text{ \AA}$ (XMM-Newton/RGS) and $\sim 1.5 - 180 \text{ \AA}$ (Chandra/HETGS and LETGS). Such spectra can only be obtained for the brightest

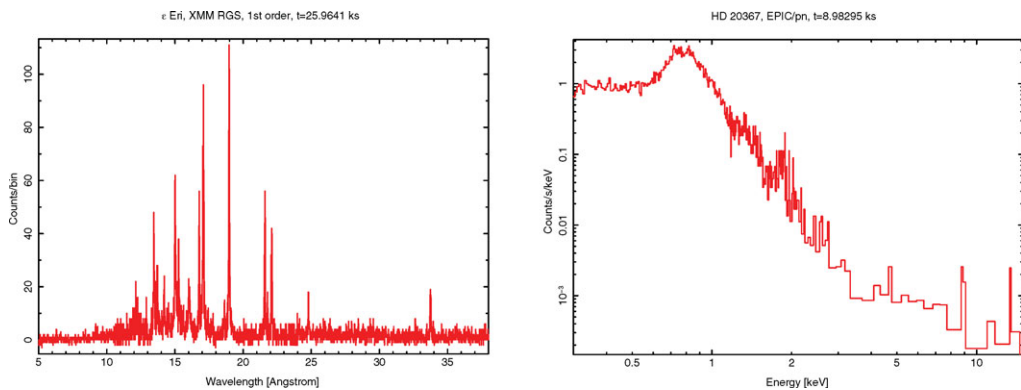


Figure 2. Real spectra observed with XMM-Newton. High resolution spectra (*left*) is only available for brightest stars. Most cases show, at most, a low-resolution spectrum (*right*).

Table 1. XMM-Newton flux of stars with exoplanets (0.12 – 2.48 keV)¹

Planet name	Spectral type (star)	Stellar distance (pc)	$\log L_X$ (erg s^{-1})	S/N (L_X)	$m \sin i$ (m_J)	a_p (a.u.)	P_{orb} (d)
14 Her b	K0V	18.10 ± 0.19	26.92	4.9	4.64	2.77	1773.4
47 Uma b	G0V	13.97 ± 0.13	<25.45	...	2.60	2.11	1083.2
47 Uma c	"	"	"	"	0.46	3.39	2190.01
β Pic b	A6V	19.30 ± 0.19	25.63	5.75	8.00	8.00	6000
Cha H α 8 b	M6.5	160	<27.87	...	18.00	1.00	1590.9
ϵ Eridani b	K2V	3.20 ± 0.01	28.20	297	1.55	3.39	2502
GQ Lup b	K7eV	140	29.45	32	21.50	103	...
HD 20367 b	G0	27.00 ± 0.79	29.30	140	1.07	1.25	500
HD 46375 b	K1IV	33.40 ± 1.19	27.16	7.3	0.25	0.04	3.02
HD 49674 b	G5V	40.70 ± 1.89	27.41	6.5	0.12	0.06	4.94
HD 50554 b	F8	31.03 ± 0.97	<26.59	...	4.90	2.38	1279
HD 62509 b	K0IIIb	10.34 ± 0.09	27.13	34	2.90	1.69	589.64
HD 70642 b	G5IV-V	29.00 ± 0.50	26.39	4.2	2.00	3.30	2231
HD 75289 b	G0V	28.94 ± 0.47	<26.16	...	0.42	0.05	3.51
HD 108147 b	F8/G0V	38.57 ± 1.03	27.39	4.2	0.26	0.10	10.90
HD 114762 b	F9V	39.46 ± 2.37	<26.61	...	11.02	0.30	83.89
HD 130322 b	K0V	30.00 ± 1.34	27.26	7.7	1.08	0.09	10.72
HD 187123 b	G5	50.00 ± 1.63	<26.80	...	0.52	0.04	3.10
HD 187123 c	"	"	"	"	1.99	4.89	3810
HD 189733 b	K1-K2	19.30 ± 0.32	28.18	93	1.13	0.03	2.22
HD 190360 b	G6IV	15.89 ± 0.16	<26.38	...	1.50	3.92	2891
HD 190360 c	"	"	"	"	0.06	0.13	17.10
HD 195019 b	G3IV-V	37.36 ± 1.24	<26.52	...	3.70	0.14	18.20
HD 209458 b	G0V	47.00 ± 2.22	<26.12	...	0.69	0.05	3.52
HD 216435 b	G0V	33.30 ± 0.81	27.74	12	1.26	2.56	1311
HD 216437 b	G4IV-V	26.50 ± 0.41	26.62	3.9	2.10	2.70	1294
HD 217107 b	G8IV	19.72 ± 0.29	<25.30	...	1.33	0.07	7.13
HD 217107 c	"	"	"	"	2.49	5.27	4210
HD 330075 b	G5	50.20 ± 3.75	26.51	3.1	0.76	0.04	3.37
NGC 2423 3 b	"	766	<29.47	...	10.60	2.10	714.3
τ Boo b	F7V	15.60 ± 0.17	28.94	317	3.90	0.05	3.31
VB 10 b	M8V	6.09 ± 0.13	25.83	20	6.40	0.36	271.56

Notes: ¹ Planet data taken from The Extrasolar Planets Encyclopedia (<http://exoplanet.eu>)

X-ray sources. Among the planet-bearing stars only two have good spectra in this range, ϵ Eri and τ Boo (Sanz-Forcada *et al.* 2004; Maggio *et al.* 2009), with a few more cases with lower quality spectra, such as HD 20367 (Table 1). In most cases we will be limited to low-resolution spectra (range $\sim 1 - 125 \text{ \AA}$), and even upper limits of the flux for the lower activity stars. The situation is even worse in the EUV range ($\sim 100 - 900 \text{ \AA}$), where no current instrumentation can observe, except for the small range covered by X-rays telescopes. The Extreme Ultraviolet Explorer (EUVE) observed a few dozens of cool stars until the year 2000, most of them at close distances. The main limitation of that mission was the absorption by the hydrogen in the interstellar medium (ISM), that becomes stronger for longer wavelengths, up to 912 \AA . Only one star with a known exoplanet was observed with EUVE, ϵ Eri (Sanz-Forcada *et al.* 2003a). The close distance of the star resulted in a good spectrum up to $\sim 400 \text{ \AA}$ (Fig. 4).

In view of this situation we have constructed a database (“X-exoplanets”) of real and synthetic spectra of stars with exoplanets. Since the real data that can be used in the models is very scant, we have created a set of high-resolution spectra constructed using coronal models. These models have been calculated using the real spectra available, and have been tested with ϵ Eri, the only case in which a good EUV spectrum is available. Most emission in both, the X-rays and EUV ranges, is produced in the corona, except for a few chromospheric and transition region lines. The database covers all the planet-bearing stars that have been observed with XMM-Newton or Chandra, and will be updated regularly as new data are incorporated. In the next lines we explain in detail how the

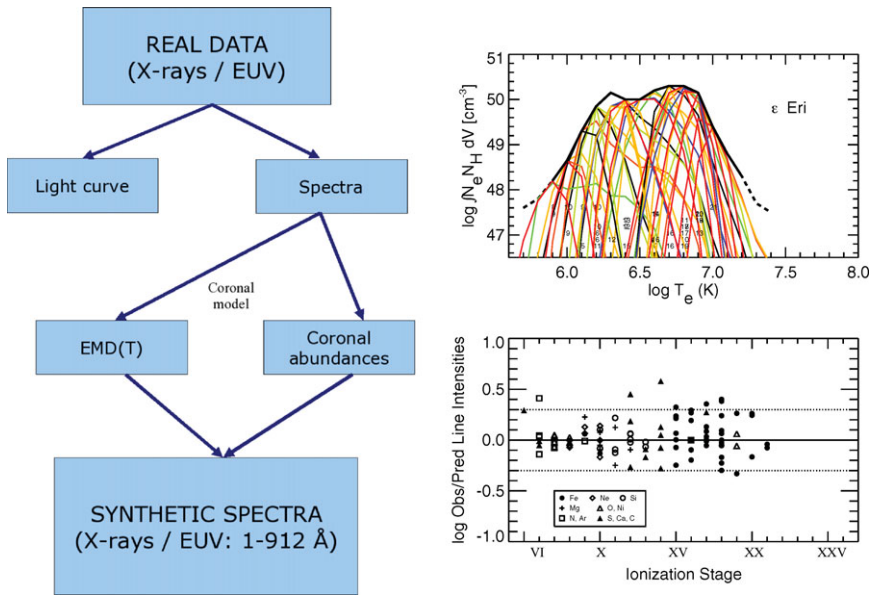


Figure 3. *Left:* schematic view of the technique employed to create the synthetic spectra from real data. *Right:* the high resolution data allow us to do a detailed reconstruction of the emission measure distribution. Synthetic spectra can be provided by use of this coronal model, in combination with the coronal abundances, also calculated during the process.

synthetic spectra are constructed, and what are the products that can be retrieved from X-exoplanets. The database can be accessed through the Spanish Virtual Observatory at the address <http://sdc.cab.inta-csic.es/xexoplanets/>

2. The database

The X-exoplanets database has the purpose to reduce all XMM-Newton and Chandra (eventually also EUVE) public data of stars with exoplanets reported, and to make these products available to the general public. We provide the light curves in different time bins (Fig. 1), and the low and high resolution spectra of the different instruments when available (Fig. 2). Some sources have not been detected, so circular regions have been selected at the expected position of the source, corrected from proper motion for the observing date; for those sources a light curve will be provided, and only an upper limit of the X-rays luminosity is included. For targets with enough statistics, the low resolution spectra have been fitted using rather simple coronal models, consisting on 1 to 3 temperature components, and a limited sample of element abundances, depending on the quality of the data (most sources can be well fitted with just 1 component). The spectra and necessary files are also provided, together with plotted spectra and residuals of the fit, and the coronal model used in the fit. For the few cases with high-resolution spectra, a detailed coronal model has been calculated using a line-based method, as described in Sanz-Forcada *et al.* (2003b), and references therein. A whole set of element abundances, and a coronal model with a $\Delta T = 0.1$ resolution are used in the fit.

The positions of the targets have been carefully calculated to improve former results. A comparison with past works show some inconsistencies with our X-ray fluxes (L_X). Since this quantity has little dependence on the exact parameters introduced in the fitting model, we attribute the discrepancy to wrong identifications of the sources. The case

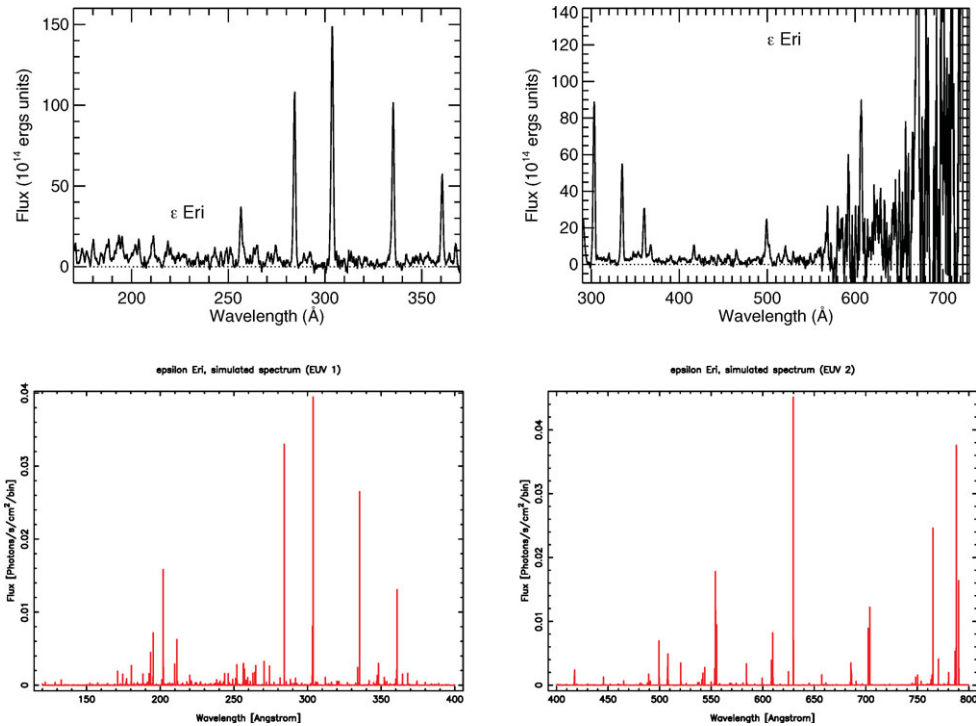


Figure 4. Real spectra (upper figures) of ϵ Eri observed with EUVE, in flux units. Note that the absorption in the interstellar medium allows very poor observations at longest EUV wavelengths. Synthetic spectra (lower figures) constructed with the coronal model successfully reproduces most spectral features of the real data.

of 47 UMa is particularly interesting. Kashyap *et al.* (2008) calculate in XMM-Newton $\log L_X = 27.13 \text{ ergs}^{-1}$. However the EPIC-pn image reveals two sources in the area of 47 UMa. The star itself ($\alpha = 10:59:28.0$, $\delta = 40:25:46$, $\log L_X < 25.45 \text{ ergs}^{-1}$) and a brighter source at $\alpha = 10:59:26.7$, $\delta = 40:26:04$, with a spectrum that resembles that of an AGN with $z \sim 0.2$ and $\log L_X \sim 43 \text{ ergs}^{-1}$ (G. Miniutti, private comm.). For the star HD 209458, that has been used in several studies because of its transiting planet, only an upper limit of $\log L_X = 26.12 \text{ ergs}^{-1}$ could be calculated, while Kashyap *et al.* (2008) cite $\log L_X = 27.02 \text{ ergs}^{-1}$, probably confused with one of the nearby sources, well identified by us with 2MASS counterparts. This problem is even worse for ROSAT detections, given the poor resolution of ROSAT/SPC.

3. Synthetic spectra

In order to have a better resolution spectra that can be used in the planetary atmospheric models, we have used our calculated coronal models to synthesize such spectra, using the atomic database APED (Smith *et al.* 2001). The method is described in Fig. 3. The central idea is that the emission in both, X-rays and EUV ranges, is originated in the corona of the star. The knowledge of the coronal model (basically the emission measure distribution, EMD, Fig. 3) and coronal abundances allows us to synthesize the whole spectral range, even if we have observations only in X-rays. The EMD is the distribution of coronal mass with temperature. The best is the model, the better will be the synthetic spectra; Low spectral resolution results only in a global fit to the spectrum and

just 1–3 components of the EMD. But the high resolution data allow us to do a detailed reconstruction of the EMD, now calculated by comparing observed line fluxes with the fluxes predicted by the combination of the atomic data and different trial EMDs (see Sanz-Forcada *et al.* 2003b, for further details).

The atomic models are quite accurate for short wavelengths, but they have not been so well tested at longer wavelengths ($\gtrsim 500 \text{ \AA}$). Besides, a few lines originated at lower temperatures (in the chromosphere or the transition region) are also present in the EUV range (most notably the He II 304 \AA line). For a few cases there are UV observations and the coronal model can be extended to lower temperatures to reproduce these lines. For other targets we are using scaling laws from the coronal EMD, based on past observations available in Sanz-Forcada *et al.* (2003a). In order to test the validity of the method we have used ϵ Eri, the case with better spectral coverage. The coronal model of this star has been calculated using Chandra and EUVE high resolution spectra (see also XMM-Newton RGS spectrum in Fig. 2). International Ultraviolet Explorer (IUE) spectra extends the EMD to the transition region and the chromosphere, so a few “cooler” lines produced below 912 \AA are properly modeled (Sanz-Forcada *et al.* 2003a, 2004). The results obtained are very promising (Fig. 4), with the models reproducing the main lines at $\lesssim 400 \text{ \AA}$ accurately. For longer wavelengths the synthetic spectra are still valid, but the quality of the real spectra falls at that range due to ISM absorption, and atomic models have not been tested so much as for shorter wavelengths.

This technique has been successfully applied to the star κ Cet (Cnossen *et al.* 2007) in order to see how the early Earth atmosphere would absorb the high energy emission from the star at the moment when life started on Earth. The use of this technique is particularly promising for transiting planets, in which some features, triggered as an effect of the incoming high-energy emission, might be observable in the transmitted spectrum of the planet.

References

- Baraffe, I., Selsis, F., Chabrier, G., *et al.* 2004, *A&A*(Letters), 419, L13
- Cecchi-Pestellini, C., Ciaravella, A., Micela, G., & Penz, T. 2009, *A&A*, 496, 863
- Cnossen, I., Sanz-Forcada, J., Favata, F., *et al.* 2007, *Journal of Geoph. Res. (Planets)*, 112, E02008
- Erkaev, N. V., Kulikov, Y. N., Lammer, H., *et al.* 2007, *A&A*, 472, 329
- Kashyap, V. L., Drake, J. J., & Saar, S. H. 2008, *ApJ*, 687, 1339
- Lammer, H., Bredehöft, J. H., Coustenis, A., *et al.* 2009, *A&AR*, 17, 181
- Lammer, H., Selsis, F., Ribas, I., *et al.* 2003, *ApJ*(Letters), 598, L121
- Maggio, A., Sanz-Forcada, J., & Scelsi, L. 2009, in *Proc. of the IAU Symposium No. 265, Chemical abundances in the Universe: connecting first stars to planets*, ed. K. Cunha, M. Spite, & B. Barbary, in press
- Micela, G. 2002, in *ASP Conf. Series, Vol. 269, The Evolving Sun and its Influence on Planetary Environments*, ed. B. Montesinos, A. Gimenez, & E. F. Guinan, p. 107
- Penz, T. & Micela, G. 2008, *A&A*, 479, 579
- Penz, T., Micela, G., & Lammer, H. 2008, *A&A*, 477, 309
- Ribas, I., Guinan, E. F., Güdel, M., & Audard, M. 2005, *ApJ*, 622, 680
- Sanz-Forcada, J., Brickhouse, N. S., & Dupree, A. K. 2003a, *ApJS*, 145, 147
- Sanz-Forcada, J., Favata, F., & Micela, G. 2004, *A&A*, 416, 281
- Sanz-Forcada, J., Maggio, A., & Micela, G. 2003b, *A&A*, 408, 1087
- Seager, S. & Sasselov, D. D. 2000, *ApJ*, 537, 916
- Smith, R. K., Brickhouse, N. S., Liedahl, D. A., & Raymond, J. C. 2001, *ApJ*(Letters), 556, L91
- Tinetti, G., Vidal-Madjar, A., Liang, M.-C., *et al.* 2007, *Nature*, 448, 169